Saishu, T., Nojima, H., & Kagawa, Y. (1986) *Biochim. Biophys. Acta 867*, 97–106.
Samama, J. P., Lee, K. M., & Biellmann, J. F. (1987) *Eur. J. Biochem. 163*, 609–617.
Sanchez-Ferrer, A., Bru, R., & Garcia-Carmona, F. (1988) *FEBS Lett. 233*, 363–366.
Schinkel, J. E., Downer, N. W., & Rupley, J. A. (1985) *Biochemistry 24*, 352–366.
Thompson, K. F., & Gierasch, L. M. (1984) *J. Am. Chem. Soc. 106*, 3648–3652.
Wheeler, C. J., & Croteau, R. (1986) *Arch. Biochem. Biophys. 248*, 429–434.
Zaks, A., & Klibanov, A. M. (1984) *Science 224*, 1249–1251.
Zaks, A., & Klibanov, A. M. (1985) *Proc. Natl. Acad. Sci. U.S.A. 82*, 3194–3196.
Zaks, A., & Klibanov, A. M. (1988a) *J. Biol. Chem. 263*, 3194–3201.
Zaks, A., & Klibanov, A. M. (1988b) *J. Biol. Chem. 263*, 8017–8021.
Zale, S. E., & Klibanov, A. M. (1986) *Biochemistry 25*, 5432–5444.

Binding Modes of Inhibitors of Ribonuclease T_1 As Elucidated by Analysis of Two-Dimensional NMR

Ichio Shimada and Fuyuhiko Inagaki*

Department of Molecular Physiology, The Tokyo Metropolitan Institute of Medical Science, 18-22 Honkomagome 3-chome, Bunkyo-ku, Tokyo 113, Japan

Received May 1, 1989; Revised Manuscript Received September 7, 1989

ABSTRACT: Aromatic proton and high field shifted methyl proton resonances of RNase T_1 complexed with Guo, 2′GMP, 3′GMP, or 5′GMP were assigned to specific amino acid residues by analyses of the two-dimensional NMR spectra in comparison with the crystal structure of the RNase T_1–2′GMP complex. These assignments were subsequently correlated to those of free RNase T_1 [Hoffmann & Rüterjans (1988) *Eur. J. Biochem. 177*, 539–560]. The spatial proximities of amino acid residues as elucidated by NOESY spectra were found to be quite similar among free RNase T_1 and the inhibitor complexes, showing that large conformational changes did not occur upon complex formation. However, small but appreciable conformational changes were induced, which were reflected by the systematic chemical shift changes of some amino acid residues in the active site. Furthermore, we confirmed that RNase T_1 contains two specific binding sites, one for the guanine base and the other for the phosphate moiety. The inhibitors are forced to adapt their conformations to fit the guanine base and the phosphate moiety to each binding site on the enzyme. This is consistent with our previous studies that 2′GMP and 3′GMP take the syn form as a bound conformation, while 5′GMP takes the anti conformation around glycosidic bonds [Inagaki et al. (1985) *Biochemistry 24*, 1013–1020]. The slow-exchange process between free and bound forms involving Tyr42 and Tyr45 was found to be specific to the recognition of the guanine base.

Ribonuclease T_1 (RNase T_1)[1] (EC 3.1.27.3) is an acidic protein (104 amino acid residues) isolated from Takadiastase, a commercial product of *Aspergillus oryzae* (Sato & Egami, 1957). RNase T_1 specifically cleaves ribonucleic acid (RNA) chains at guanylic acid residues. Rigorous recognition of a guanine base by RNase T_1 is a typical example of an RNA–protein interaction. A number of studies have been made to elucidate the specific interaction and the enzymatic mechanism of RNase T_1. From chemical and kinetic studies, amino acid residues located in the active site have been suggested: His40, His92, Glu58, and Arg77 (Takahashi & Moore, 1982; Osterman & Walz, 1979). Nuclear magnetic resonance (NMR) analyses also have given valuable information on this point (Rüterjans & Pongs, 1971; Arata et al., 1979; Inagaki et al., 1981, 1985; Kyogoku et al., 1982; Hoffmann & Rüterjans, 1988). Recently, the crystal and molecular structures of RNase T_1–2′GMP (Heinemann & Saenger, 1982; Sugio et al., 1985a, 1988; Arni et al., 1988) and RNase T_1–3′GMP (Sugio et al., 1985b) have been elucidated by X-ray analysis. In the present study, we report the analysis of the NMR spectra of RNase T_1 complexed with inhibitors by the 2D NMR method. By comparing the results of the NOE experiments with the molecular structure obtained by the X-ray analysis, the aromatic proton and the high field shifted methyl proton resonances in the RNase T_1–inhibitor complexes were assigned to the specific amino acid residues. These assignments were subsequently compared with those obtained by the analysis of free RNase T_1 (Hoffmann & Rüterjans, 1988). On the basis of the present assignments and the conformational properties of the inhibitors, the binding modes of the inhibitors to RNase T_1 were discussed.

Experimental Procedures

RNase T_1 was prepared from Takadiastase by affinity chromatography (Kanaya & Uchida, 1981). The enzymatic

* Author to whom correspondence should be addressed.

[1] Abbreviations: RNase T_1, ribonuclease T_1; Guo, guanosine; 2′GMP, guanosine 2′-monophosphate; 3′GMP, guanosine 3′-monophosphate; 5′GMP, guanosine 5′-monophosphate; DQF-COSY, double quantum filtered correlated spectroscopy; HOHAHA, homonuclear Hartmann–Hahn spectroscopy; NOE, nuclear Overhauser effect; NOESY, nuclear Overhauser effect spectroscopy; 2D NMR, two-dimensional NMR; CIDNP, chemically induced dynamic nuclear polarization; 1D NMR, one-dimensional NMR.

0006-2960/90/0429-757$02.50/0

activity of purified RNase T_1 was about 1.6×10^4 units/mg according to the assay method of Takahashi (1961b). Guo, 2′(3′)GMP, and 5′GMP were purchased from Kyowa Hakko Co. 2′GMP and 3′GMP were isolated from 2′(3′)GMP by use of a Dowex 1 × 2 column (Hurlbert, 1957). The 500-MHz ^{1}H NMR spectra were recorded on a JEOL JNM-GX500 spectrometer at 37 °C. The NMR samples of RNase T_1 were dissolved in ^2H_2O at a concentration of ca. 1 mM. Labile OH and NH hydrogen atoms of RNase T_1 were completely exchanged with deuterium atoms by incubating the sample in ^2H_2O solution at pH 7.5 for about 10 min at 50 °C (Inagaki et al., 1981). The pH values of all the sample solutions were adjusted to pH ca. 5.5 by the addition of 1 M ^{2}HCl or NaO^{2}H in the present study. The pH values (direct pH meter readings) were measured directly in a 5-mm NMR tube by use of a Radiometer PHM-84 pH meter. 2,2-Dimethyl-2-silapentane-5-sulfonate (DSS) was used as an internal standard of chemical shifts. DQF-COSY (Piantini et al., 1982), HOHAHA (Bax & Davis, 1985), and NOESY (Jeener et al., 1979) spectra were measured in the phase-sensitive mode (States et al., 1982). A total of 512 blocks were acquired with data points of 2048. The obtained data matrix was zero-filled once along t_1 direction to the final data matrix of 1K × 1K. The shifted sine bell was used for the apodization function. Mixing times were set to be 45 and 150 ms for the measurements of HOHAHA and NOESY spectra, respectively. For 1D NOE measurements, irradiation power and irradiation time were set to minimize the spin diffusion effects. We usually used an irradiation time of 0.5 s. Eight scans of on-resonance and off-resonance irradiation were alternatively accumulated up to a total of 512 scans, respectively. Negative NOE enhancements were extracted by use of the difference method (Richard & Wüthrich, 1978).

Results

RNase T_1 contains three histidine residues (H27, H40, and H92), four phenylalanine residues (F48, F50, F80, and F100), nine tyrosine residues (Y4, Y11, Y24, Y38, Y42, Y45, Y56, Y57, and Y68), and one tryptophan residue (W59) (Takahashi, 1961a). Upon inhibitor binding, some of the aromatic proton and the high field shifted methyl proton resonances of RNase T_1 were significantly shifted, in addition to the C2 and C4 proton resonances of three histidine residues, suggesting that these residues are involved in the binding of the inhibitors (Rüterjans & Pongs, 1971; Arata et al., 1979; Inagaki et al., 1981, 1985). Actually, the X-ray crystal structure of the RNase T_1–2′GMP complex shows that the binding of 2′GMP by RNase T_1 appears to involve a peptide segment comprising Y42-N43-N44-Y45-E46-G47-F48-D49-F50 and by some aromatic and methyl group bearing amino acid residues (Sugio et al., 1988; Hakoshima et al., 1988; Arni et al., 1988). To elucidate the interaction of RNase T_1 with inhibitors, the assignments of the aromatic proton and the high field shifted methyl proton resonances of RNase T_1 and its inhibitor complexes are essential. Recently, sequence-specific resonance assignment of free RNase T_1 was made (Hoffmann & Rüterjans, 1988). In the present study, we focused on analysis of the NMR spectra of RNase T_1–inhibitor complexes. Figure 1a shows the 500-MHz ^{1}H NMR spectrum of free RNase T_1 in the aromatic and the high field shifted methyl proton regions with the assignments obtained by Hoffmann and Rüterjans (1988). Since significant spectral changes of RNase T_1 were observed upon binding of 2′GMP (Figure 1b), a small amount of the 2′GMP solution (50 mM, pH 5.5) was successively added to the sample solution to follow the changes of the chemical shifts of these proton resonances (Figure 2). The pH values of the sample solutions were checked before and after the NMR measurements and found to be 5.5 ± 0.1. The binding of 2′GMP to RNase T_1 is maximal around this pH value. Although most of resonances gradually changed their chemical shifts upon increasing the molar ratio of 2′GMP to RNase T_1, some of the resonances (shown by shading in Figure 2a) decreased their intensities and disappeared. Instead, new peaks appeared, which are shown by shading in Figure 2e. Since the simple titration study could not give rigorous assignments of such resonances, we started to assign the aromatic proton and the high field shifted methyl proton resonances of RNase T_1–2′GMP by comparing the analysis of the 2D NMR spectra with the molecular structure obtained by X-ray analysis.

Assignment of the Aromatic Proton and High Field Shifted Methyl Proton Resonances of the RNase T_1–2′GMP Complex. Assignment of the aromatic proton and the high field shifted methyl proton resonances of RNase T_1 in the 2′GMP-bound form was made by using DQF-COSY, HOHAHA, and NOESY in the presence of 2′GMP at a molar ratio of 3.0 and at pH 5.5. At this condition, RNase T_1 was saturated with the inhibitor. The DQF-COSY and HOHAHA spectra of the RNase T_1–2′GMP complex are shown in the lower left and upper right halves of Figure 3, respectively. The spin systems of six tyrosine aromatic protons (Ya, Yb, Yc, Yd, Ye, and Yf) were easily identified by the cross-peak patterns of the DQF-COSY spectrum and are enclosed by boxes. The aromatic proton resonances of one tyrosine residue (Yg) showed a singlet line due to degeneracy of the chemical shifts of the C2,6 and C3,5 proton resonances. However, the remaining two tyrosine residues were not detected, possibly due to broadening of the resonances. One of these tyrosine residues (Yh) was assigned from the analysis of the NOESY spectrum. The spin systems of four phenylalanine residues (Fa, Fb, Fc, and Fd) and a single tryptophan residue (W59) were also identified by 2D HOHAHA in combination with DQF-COSY (Figure 3). The spin systems of the aromatic proton resonances of RNase T_1–2′GMP thus identified are shown Figure 1b. The high field shifted methyl proton resonances were also assigned to the specific amino acid types through analysis of the DQF-COSY and HOHAHA spectra (Figure 1b), which were consistent with our previous assignment (Inagaki et al., 1985).

Sequence-Specific Resonance Assignment. The sequence-specific resonance assignment of those aromatic proton and high field shifted methyl proton resonances was subsequently made as compared to the results of the NOESY spectrum and the molecular structure of the RNase T_1–2′GMP complex elucidated by X-ray crystallography (Sugio et al., 1988; Arni et al., 1988). Panels a and b of Figure 4 show the NOESY spectrum of the RNase T_1–2′GMP complex in the aromatic proton region and the cross-peak region between the aromatic and the high field shifted methyl protons, respectively. From the analysis of the NOESY cross-peaks, the spatial proximities of the aromatic and the high field shifted methyl-bearing amino acid residues were elucidated, as shown in Figure 5. Note that three histidine residues were sequence-specifically assigned (Arata et al., 1979; Inagaki et al., 1981), and tryptophan was readily assigned to W59 because RNase T_1 contains a single tryptophan residue. RNase T_1 contains two isoleucine residues (I61 and I90). One of two isoleucine residues (Ia) was found to be located in a hydrophobic box surrounded by three phenylalanine residues (Fb, Fc, and Fd) and one tyrosine residue (Yh), while the other isoleucine residue is located in close proximity to one tyrosine residue

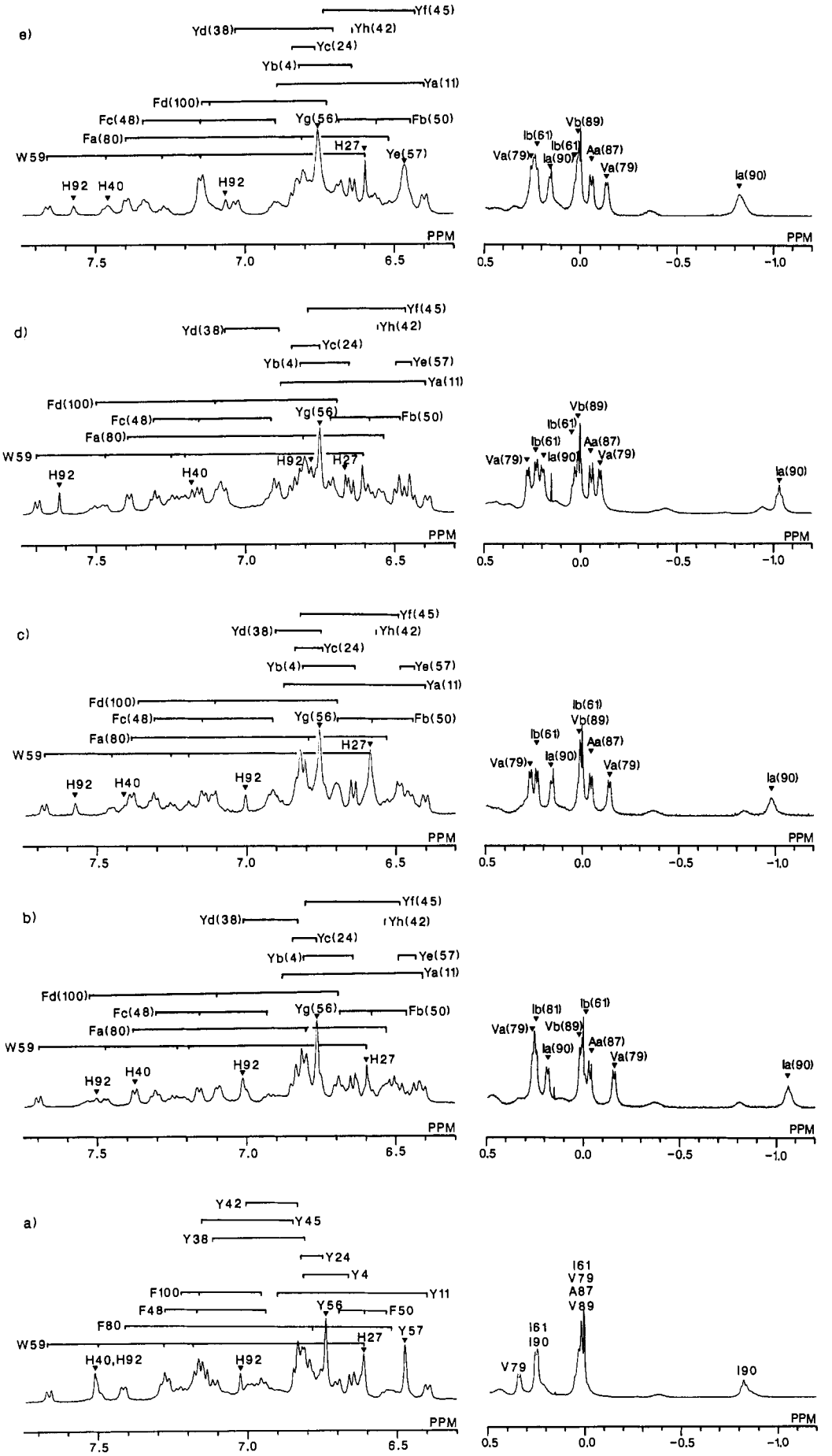

FIGURE 1: 500-MHz ^1H NMR spectra of (a) RNase T_1, (b) RNase T_1–2′GMP (3.0), (c) RNase T_1–3′GMP (5.0), (d) RNase T_1–5′GMP (5.0), and (e) RNase T_1–Guo (5.0) at pH 5.5 and 37 °C in the aromatic and the high field shifted methyl proton regions with the assignment of the proton resonances. The molar ratios of the inhibitors to RNase T_1 are given in parentheses.

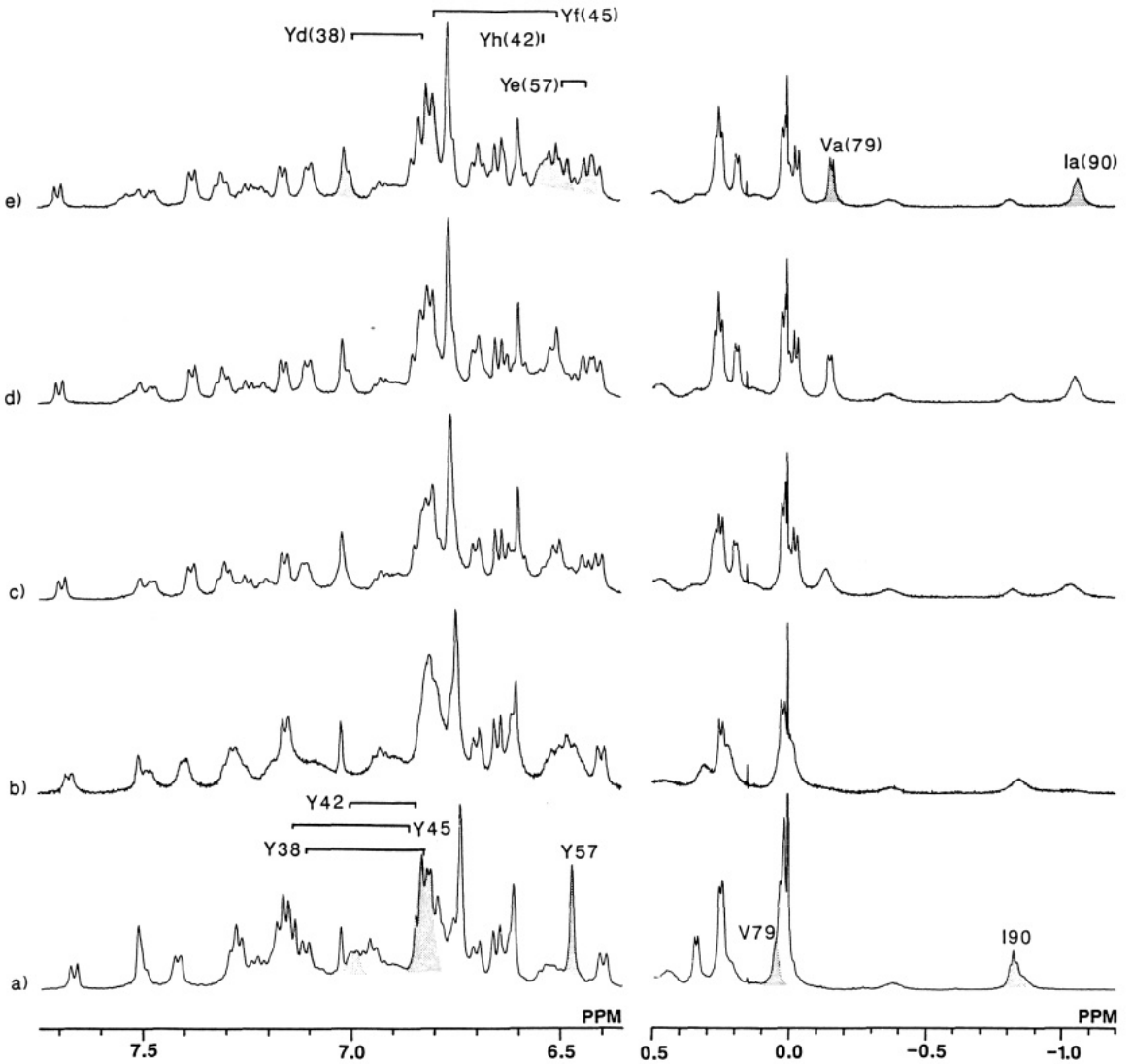

FIGURE 2: Dependence of the chemical shifts of the aromatic and the high field shifted methyl proton resonances upon the molar ratio of 2′GMP to RNase T_1 at pH 5.5 and 37 °C. Aliquots of a 50 mM solution of 2′GMP at pH 5.5 were successively added to the sample solution. The molar ratio of 2′GMP to RNase T_1 in each spectrum is (a) 0.0, (b) 0.2, (c) 0.6, (d) 0.8, and (e) 3.0. The resonances with shading show a slow-exchange process upon binding of 2′GMP.

(Ya). Compared with the molecular structure of the RNase T_1–2′GMP complex (Sugio et al., 1988; Hakoshima et al., 1988; Arni et al., 1988), I90 is actually located in the hydrophobic box as shown in Figure 5a. The spatial proximities of these aromatic and methyl-bearing amino acid residues are in good agreement with those deduced from NOESY experiment, and thus, the following assignments were established: Ia to I90, Yh to Y42, Yg to Y56, Fb to F50, Fc to F48, Fd to F100, Aa to A87, and Va to V79. Importantly, these residues form the part of the hydrophobic box adjacent to the active site of RNase T_1. The present NMR study shows that the active site structure of the RNase T_1–2′GMP complex in aqueous solution is in good agreement with that obtained by X-ray analysis. In a similar manner, other spatial proximities of the aromatic and methyl-bearing amino acid residues were searched (Figure 5b–5e). Compared with the spatial proximities elucidated by NMR and X-ray analysis again, the following assignments were established: Fa to F80, Yc to Y24, Ye to Y57, Yd to Y38, Ya to Y11, Ib to I61, Yb to Y4, and Vb to V89. The assignments of the aromatic proton and the high field shifted methyl proton resonances of RNase T_1–2′GMP are summarized in Figure 1b. Since these residues are located over the protein, the similarity of the spatial proximities of these residues as elucidated in the present NMR study and in the crystal structure strongly supports that the structure of RNase T_1–2′GMP in the crystalline state is also maintained in solution structure.

It is to be noted that the aromatic proton resonances of Y38, Y42, and Y45 and I90 δ and V79 γ methyl proton resonances were significantly broadened even on the addition of a 0.2 molar ratio of 2′GMP to RNase T_1 and new peaks appeared at a high molar ratio of 2′GMP, as shown by shading in Figure 2. It is also to be noted that Y57 showed a slow-exchange process from a singlet to an AA′BB′ pattern. This is a characteristic of a slow-exchange process which occurs between the free and bound states compared to the chemical shift time scale (Wüthrich, 1976). The present results show that these residues are located in different chemical environments between the two states. In addition to these proton resonances, the aromatic proton resonances of F100 and the methyl proton resonance of A87 changed their chemical shifts upon binding of 2′GMP, while those of the aromatic proton resonances of Y4, Y11, Y24, Y56, F48, F50, and W59 and the methyl proton resonances of I61 and V89 showed only small changes.

In a similar manner, the aromatic proton and the high field shifted methyl proton resonances of RNase T_1–3′GMP, RNase T_1–5′GMP, and RNase T_1–Guo were assigned to the specific amino acid residues and are summarized in Figure 1c–e. NOE

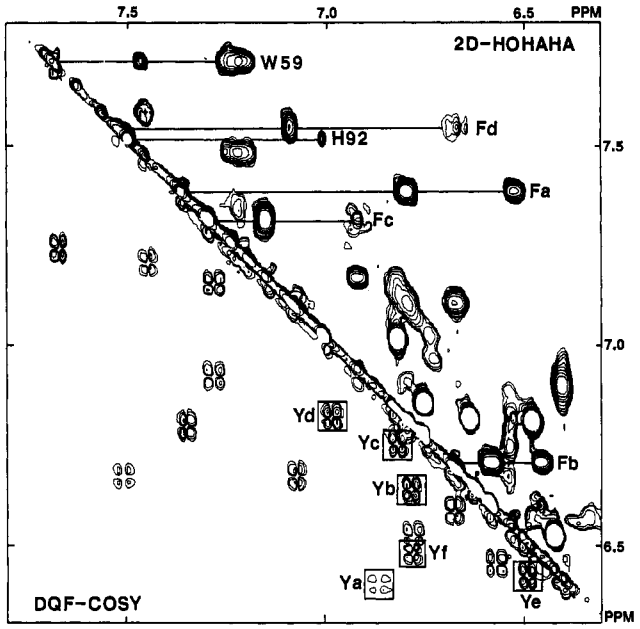

FIGURE 3: DQF-COSY and HOHAHA spectra of RNase T_1–2′GMP in the lower left and upper right halves, respectively, at pH 5.5 and 37 °C. The molar ratio of 2′GMP to RNase T_1 is 3.0. The cross-peaks due to C2,6 and C3,5 protons of tyrosine residues are boxed in the DQF-COSY spectrum. The spin systems of the phenylalanine and the tryptophan residues are connected by solid lines in the HOHAHA spectrum.

connectivities observed for free RNase T_1 and the RNase T_1–inhibitor complexes are shown in Figure 6. In addition, distance connectivities calculated from the crystal structure of RNase T_1–2′GMP are also shown. These maps are quite similar, supporting that the large conformational changes were not induced upon binding of the inhibitors. Thus, it is concluded that the solution structures of free RNase T_1 and the RNase T_1–inhibitor complexes can be discussed on the basis of the crystal structure of RNase T_1–2′GMP. However, it is to be noted that the NOE connectivities between (Y42, Y48) and (F50, Y56) were not observed for free RNase T_1 (Figure 6c; Hoffmann & Rüterjans, 1988). These residues are located on the binding loop of the guanine base, so that a small but appreciable conformational change occurs in the loop region upon binding of the inhibitors.

Behaviors of the Aromatic Proton Resonances Due to Inhibitor Binding. The aromatic proton resonances were classified into several groups according to the spectral behavior upon inhibitor binding. Y42 and Y45 evidenced a slow-exchange process compared to the chemical shift time scale for all inhibitors in the present study. Y38 and Y57 also showed a slow-exchange process for 2′GMP, 3′GMP, and 5′GMP binding but not for Guo binding. F100 showed a large change of chemical shifts upon binding of the inhibitors with a fast-exchange process, while other aromatic proton resonances (Y4, Y11, Y24, Y56, F48, F50, F80, and W59) did not show any appreciable chemical shift changes. In Figure 7, we compare the chemical shifts of some of the aromatic proton and I90 δ methyl proton resonances of the RNase T_1–inhibitor complexes with reference to the chemical shifts of those of free RNase T_1. Since global conformational changes were not induced upon inhibitor bindings, these changes were due to the direct interaction with inhibitors and/or local conformational changes.

Discussion

In the present study, it was shown that the active site structure of the RNase T_1–2′GMP complex in solution was very similar to that in the crystalline state. On the basis of the crystal structure (Heinemann & Saenger, 1982; Sugio et al., 1985a, 1988; Arni et al., 1988), the aromatic proton and the high field shifted methyl proton resonances in the bound form with 2′GMP were assigned to the specific amino acid residues and were correlated to those in the free form (Hoffmann & Rüterjans, 1988). The spatial proximities elucidated in the present study were quite similar for free and inhibitor-bound RNase T_1, showing that the binding of the inhibitors does not induce global conformational change of the enzyme (Figure 6). However, small but appreciable conformational change was induced around the binding loop upon binding of inhibitors, which was elucidated by the chemical shift changes of some of the aromatic and methyl proton resonances and the results of the NOESY experiments (Figure 6).

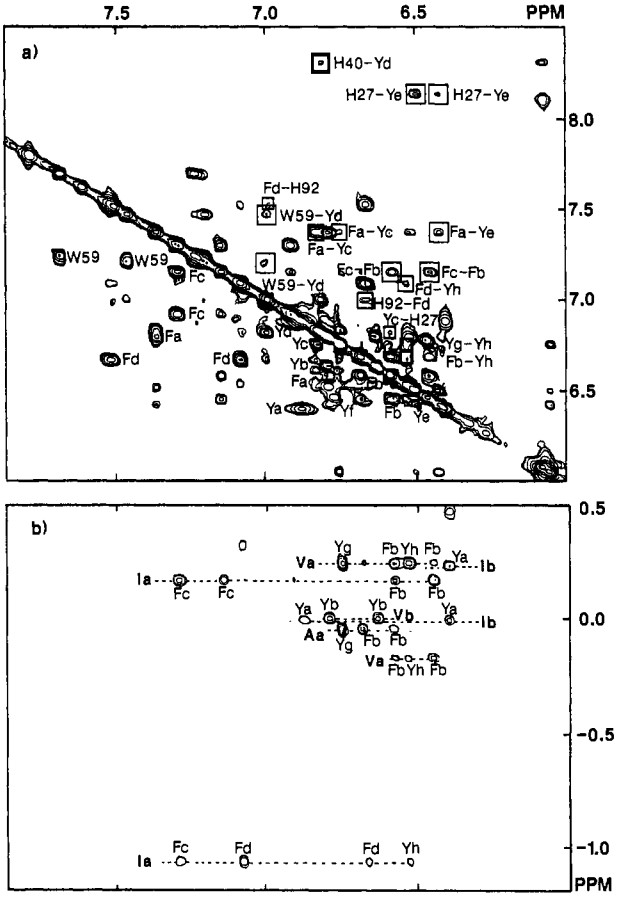

FIGURE 4: NOESY spectra of RNase T_1–2′GMP in (a) the aromatic proton region and (b) the cross-peak region of the aromatic and the high field shifted methyl protons with the assignment of the cross-peaks. NOESY cross-peaks due to interresidues are boxed in the upper right half, and those due to intraresidues are labeled in the lower left half of the aromatic region. NOE cross-peaks due to the aromatic and the methyl groups are connected by dotted lines in (b).

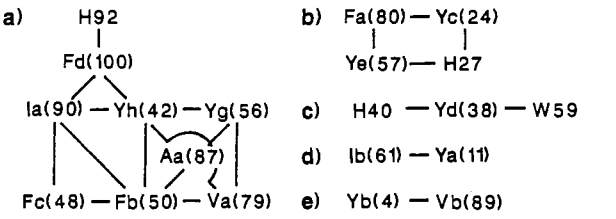

FIGURE 5: Spatial proximities of the aromatic and high field shifted methyl-bearing amino acid residues as elucidated from NOESY experiments of RNase T_1–2′GMP. Residue numbers shown in parentheses are identified from the spatial proximities calculated from the crystal structure of RNase T_1–2′GMP.

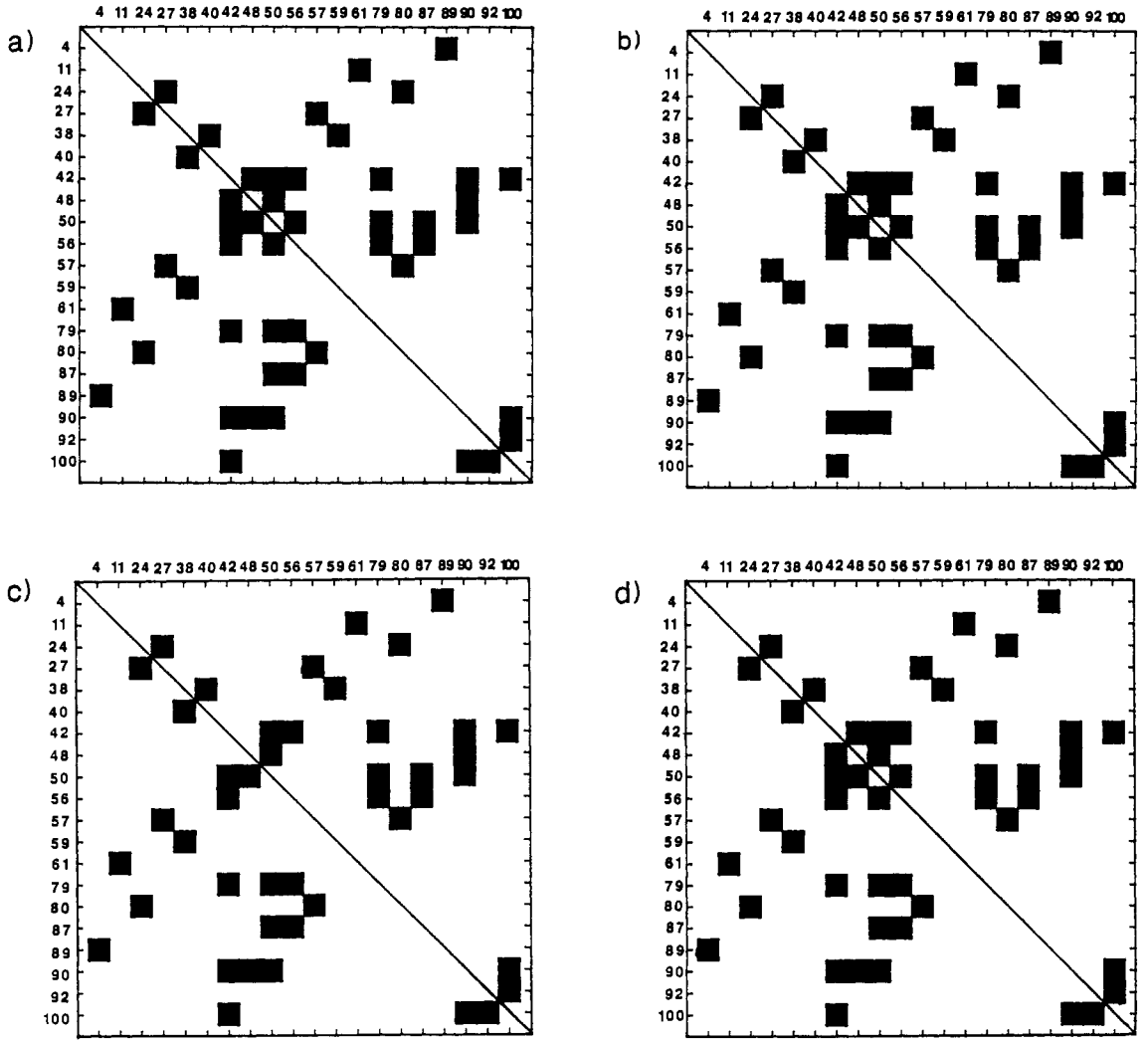

FIGURE 6: (a) Distance connectivities of the aromatic and the high field shifted methyl-bearing amino acid residues obtained from the crystal structure of RNase T_1–2′GMP. (b–f) NOE connectivities of the aromatic and the high field shifted methyl-bearing amino acid residues as elucidated from NOESY. (b) RNase T_1–2′GMP, (c) RNase T_1, (d) RNase T_1–3′GMP (the same NOE connectivities were obtained for RNase T_1–5′GMP and RNase T_1–Guo). Numbers on both axes correspond to the amino acid residues Y4, Y11, Y24, H27, Y38, H40, Y42, F48, F50, Y56, Y57, W59, I61, V79, F80, A87, V89, I90, H92, and F100.

In all inhibitor bindings, Y42 and Y45 showed a slow-exchange process, between free and bound states, where the exchange rate was estimated to be slower than 10 ms. It is generally difficult to identify that the slow-exchange process reflects either a binding process or a conformational change. However, since binding of inhibitors induced a small but appreciable conformational change in the binding loop (Figure 6), it is reasonable that the slow-exchange process accompanied the conformational change. The conformational change induced by the binding of inhibitors is also supported from the recent photo-CIDNP experiment, showing that the exposed Y45 in the free state is buried in the RNase T_1–2′GMP complex (Nagai et al., 1985). According to the crystal structure of the RNase T_1–2′GMP complex, the aromatic ring of Y45 hangs over the guanine base which sits on the aromatic ring of Y42. The high-field shift of the Y42 and Y45 aromatic proton resonances upon binding of 2′-GMP is possibly due to the ring current shift of the guanine base (Figure 7). Thus, the slow-exchange process observed for Y42 and Y45 in the binding of the inhibitors possibly accompanies the slow conformational change of the guanine-binding loop, which may be essential for the specific recognition of the guanine base by RNase T_1. The guanine-binding loop found in the RNase T_1–2′GMP complex comprises Y42-N43-N44-Y45E-46-G47-F48-D49-F50, where the amide protons of the backbone of N43 and N44 form hydrogen bonds with the guanine base in addition to the stacking of the guanine base with Y42 and Y45.

Binding Site of the Phosphate Moiety. The crystal structure of the RNase T_1–2′GMP complex shows that the phosphate moiety is located in close proximity to the guanidinium group of R77. Y38, I90, and F100 are located in the vicinity of the phosphate binding site, so that these residues are good probes for studying the effects of the binding of the phosphate moiety to RNase T_1. Upon binding of 2′GMP to RNase T_1, Y38 and I90 showed a slow-exchange process accompanied by the large chemical shift changes of F100 (Figure 2a,e). Similar observations were made for RNase T_1–3′GMP, RNaseT_1–5′GMP, and RNase T_1–Guo which are summarized in Figure 7. In addition to Y38, F100, and I90, Y57 was also found to be sensitive to the presence of the phosphate moiety. Y57 showed a slow-exchange process upon binding of the phosphate group bearing inhibitors. According to the crystal structure of RNase T_1–2′GMP, Y57 does not directly interact with 2′GMP but is located in the periphery of the active site. By comparison with the chemical shift behaviors from the free to the bound states of RNase T_1, we concluded that Y38, Y57, F100 (especially H4 proton), and I90 were good probes for detecting the small conformational changes around the active site induced by the binding of the phosphate moiety, which

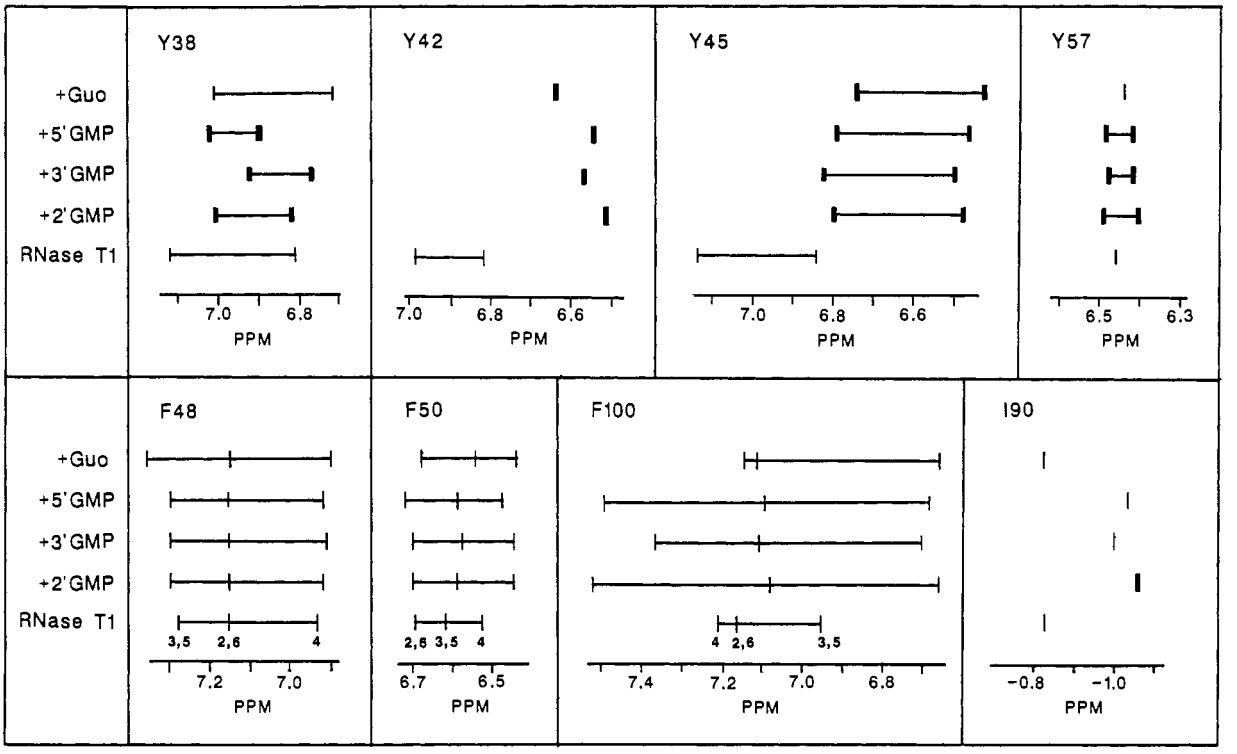

FIGURE 7: Comparison of the chemical shifts of the aromatic proton resonances of Y38, Y42, Y45, Y57, F48, F50, and F100 and the I90 δ methyl proton resonance of RNase T_1, RNase T_1–2′GMP, RNase T_1–3′GMP, RNase T_1–5′GMP, and RNase T_1–Guo at pH 5.5 and 37 °C. The resonances with bold lines show a slow-exchange process upon binding of the inhibitors. C2,6H of Y42 was not observed.

could not be detected by the NOE experiments. In the crystal structure of RNase T_1–3′GMP, the electron density of the phosphate and the ribose moiety is smeared out, possibly due to the spatial disorder of the crystals (Sugio et al., 1985b). As shown in Figure 7, the chemical shift behaviors of the Y38, Y57, F100, and I90 proton resonances upon the binding of 3′GMP were similar to those upon the binding of 2′GMP. This supports that the phosphate groups of 2′GMP and 3′GMP bind to RNase T_1 in a similar position. This result leads to the conclusion that RNase T_1 contains the binding sites for the guanine base, which is sensed by Y42, Y45, V79, and A87, and for the phosphate moiety, which is sensed by Y38, Y57, F100, and I90, respectively, but not for the ribose moiety. Actually, in the case of the molecular structure of RNase T_1–2′GMP, the ribose moiety does not interact with RNase T_1 (Sugio et al., 1988; Arni et al., 1988).

Binding Mode of 5′GMP. It is to be noted that the induced chemical shifts of the Y42, Y45, V79, A87, Y38, Y57, F100, and I90 proton resonances upon binding of 5′GMP were quite similar to those upon binding of 2′GMP and 3′GMP (Figure 7), suggesting that the guanine bases and the phosphate groups of these inhibitors bind to similar sites of RNase T_1. This supports the possibility that there is a conformational difference among those inhibitors around the glycosidic linkages (Inagaki et al., 1985). Thus, we compared the conformations of the guanosine moieties of 3′GMP and 5′GMP as bound to RNase T_1 using the 1D difference NOE method. In addition to NOE between H1′ and H8, NOEs among H8 and other sugar protons were studied in the present study, which were assigned by the analysis of the DQF-COSY spectra. In the case of RNase T_1–3′GMP, the irradiation of H8 induced large NOE on H1′ and only negligible NOE enhancements on other sugar protons. Converse irradiation of H1′ showed a large NOE enhancement again on H8, showing that the conformation taken by the glycosidic bond in 3′GMP is syn as bound to RNase T_1. In the case of RNase T_1–5′GMP, a small NOE enhancement was observed for H1′ but appreciably larger NOE enhancements were observed for H2′ and H3′ upon irradiation of H8. Converse irradiation of H1′ gave again negligible NOE enhancement on H8. These results corroborate the previous conclusion that the conformation taken by the glycosidic bond in 5′GMP is high-anti rather than syn. Moreover, from the observed NOE enhancements, the sugar moiety of 5′GMP takes the 3′endo conformation. The anti conformation around the glycosidic bond in 5′GMP is forced to adapt the guanine base and the phosphate group to the binding sites of RNase T_1 similar to those observed for RNase T_1–2′GMP. The present result suggests that RNase T_1 has no intrinsic binding site for the phosphate moiety at the 5′-position. The conformation change around the glycosidic bond in 5′GMP is possible only when the sugar moiety does not form hydrogen bonds with RNase T_1. Actually, the strong binding of 9-(2-hydroxyethyl)guanine 2′-phosphate (Takahashi, 1982) implies that the ribose of the guanine nucleotide inhibitors appears to serve as a spacer between the guanine base and the phosphate group. However, the ribose rings of RNA chains as substrates should be essential for the proper orientation of the recognition site and the catalytic site.

ACKNOWLEDGMENTS

We are grateful to Prof. Ken-ichi Tomita, Dr. Toshio Hakoshima, and Dr. Satoshi Nishikawa of Osaka University for their helpful discussions.

Registry No. Guanylribonuclease, 9026-12-4.

REFERENCES

Arata, Y., Kimura, S., Matsuo, H., & Narita, K. (1979) *Biochemistry 18*, 18–24.

Arni, R., Heinemann, U., Tokuoka, R., & Saenger, W. (1988) *J. Biol. Chem. 263*, 15358–15368.

Bax, A., & Davis, D. G. (1985) *J. Magn. Reson. 65*, 355–360.

Hakoshima, T., Toda, S., Sugio, S., Tomita, K., Nishikawa, S., Morioka, H., Fuchimura, K., Kimura, T., Uesugi, S.,

Ohtsuka, E., & Ikehara, M. (1988) *Protein Eng. 2*, 55-61.
Heinemann, U., & Saenger, W. (1982) *Nature (London) 299*, 27-31.
Hoffmann, E., & Rüterjans, H. (1988) *Eur. J. Biochem. 177*, 539-560.
Hurlbert, R. B. (1957) *Methods Enzymol. 3*, 785-805.
Inagaki, F., Kawano, Y., Shimada, I., Takahashi, K., & Miyazawa, T. (1981) *J. Biochem. (Tokyo) 89*, 1185-1195.
Inagaki, F., Shimada, I., & Miyazawa, T. (1985) *Biochemistry 24*, 1013-1020.
Jeener, J., Meier, B. H., Bachmann, P., & Ernst, R. R. (1979) *J. Chem. Phys. 71*, 4546-4553.
Kanaya, S., & Uchida, T. (1981) *J. Biochem. (Tokyo) 89*, 591-597.
Kyogoku, Y., Watanabe, M., Kainosho, M., & Oshima, T. (1982) *J. Biochem. (Tokyo) 91*, 675-679.
Nagai, H., Kawata, Y., Hayashi, F., Sakiyama, F., & Kyogoku, Y. (1985) *FEBS Lett. 189*, 167-170.
Osterman, H. L., & Walz, F. G., Jr. (1979) *Biochemistry 18*, 1984-1988.
Piantini, U., Sorensen, O. W., & Ernst, R. R. (1982) *J. Am. Chem. Soc. 104*, 6800-6801.
Richarz, R., & Wüthrich, K. (1978) *J. Magn. Reson. 30*, 147-150.
Rüterjans, R., & Pongs, O. (1971) *Eur. J. Biochem. 18*, 313-318.
Sato, K., & Egami, F. (1957) *J. Biochem. (Tokyo) 44*, 753-767.
States, D. J., Haberkorn, R. A., & Reuben, D. J. (1982) *J. Magn. Reson. 48*, 286-292.
Sugio, S., Amisaki, T., Ohishi, H., Tomita, K., Heinemann, U., & Saenger, W. (1985a) *FEBS Lett. 181*, 129-132.
Sugio, S., Oka, K., Ohishi, H., Tomita, K., & Saenger, K. (1985b) *FEBS Lett. 183*, 115-118.
Sugio, S., Amisaki, T., Ohishi, H., & Tomita, K. (1988) *J. Biochem. (Tokyo) 103*, 354-366.
Takahashi, K. (1961a) *J. Biol. Chem. 240*, 4117-4119.
Takahashi, K. (1961b) *J. Biochem. (Tokyo) 60*, 239-245.
Takahashi, K. (1972) *J. Biochem. (Tokyo) 72*, 1469-1481.
Takahashi, K., & Moore, S. (1982) *Enzymes* (Boyer, P. D., Ed.) pp 453-468, Academic Press, New York and London.
Wüthrich, K. (1976) *NMR in Biological Research: Peptides and Proteins*, North-Holland, Amsterdam, Oxford/American Elsevier, New York.

Effect of Changing the Detergent Bound to Bovine Cytochrome *c* Oxidase upon Its Individual Electron-Transfer Steps†

Surendra N. Mahapatro‡ and Neal C. Robinson*
Department of Biochemistry, The University of Texas Health Science Center, 7703 Floyd Curl Drive, San Antonio, Texas 78284-7760

Received June 27, 1989; Revised Manuscript Received September 6, 1989

ABSTRACT: The influence of the detergent environment upon individual electron-transfer rates of cytochrome *c* oxidase was investigated by stopped-flow spectrophotometry. The effects of three detergents were studied: lauryl maltoside, which supports a high turnover number (TN = 350 s^{-1}), *n*-dodecyl octaethylene glycol monoether ($C_{12}E_8$), which supports an intermediate TN (150 s^{-1}), and Triton X-100 in which oxidase is nearly inactive (TN = 2-3 s^{-1}). Under limited turnover conditions (cytochrome *c*:cytochrome *c* oxidase ratio = 1:1 to 8:1), the rate of oxidation of cytochrome *c* was measured and compared with the fast reduction of cytochrome *a* and its relatively slow reoxidation. Two reducing equivalents of cytochrome *c* were rapidly oxidized in a burst phase; the remaining two to six equivalents were oxidized more slowly, concurrent with the reoxidation of cytochrome *a*; i.e., the percent reduced cytochrome *a* reflects the percent reduced cytochrome *c*. With the resting enzyme, the bimolecular reaction between reduced cytochrome *c* and cytochrome *a* was rapid, was insensitive to the detergent environment, and was not the rate-limiting step in the presence of any detergent. The rate of internal electron transfer from cytochrome *a* to cytochrome a_3 in the resting enzyme was slow and only slightly affected by the detergent environment: 1.0-1.1 s^{-1} in Triton X-100, 5-7 s^{-1} in $C_{12}E_8$, and 5-12 s^{-1} in lauryl maltoside. With the pulsed enzyme, the intramolecular electron transfer between cytochrome *a* and cytochrome a_3 increased 4-5-fold in the lauryl maltoside enzyme but did not increase in the Triton X-100 enzyme (intermediate values were obtained with the $C_{12}E_8$ enzyme). We conclude that cytochrome *c* oxidase acquires the pulsed conformation only in those detergents that support high TN's, e.g., lauryl maltoside and $C_{12}E_8$, but it is locked in the resting conformation in those detergents which result in low TN's, e.g., Triton X-100.

Cytochrome *c* oxidase is an integral membrane protein complex that spans the inner mitochondrial membrane. The complex catalyzes the four-electron reduction of oxygen to water by four transmembrane electron transfers from reduced cytochrome *c*. In steady-state experiments, the turnover number (TN)[1] of the enzyme is sensitive to the apolar envi-

† This research was supported by National Institutes of Health Grant GM24795.
* To whom correspondence should be addressed.
‡ Present address: Department of Chemistry, Regis College, Denver, CO 80221.

[1] Abbreviations: $C_{12}E_8$, *n*-dodecyl octaethylene glycol monoether; LM, lauryl maltoside (dodecyl β-D-maltopyranoside); TN, enzymatic turnover number; TX, Triton X-100; Tris-acetate buffer, tris(hydroxymethyl)-aminomethane base titrated to the appropriate pH with acetic acid; TMPD, *N,N,N',N'*-tetramethyl-*p*-phenylenediamine; $C_{12}E_8$-enzyme, cytochrome *c* oxidase with bound $C_{12}E_8$; LM-enzyme, cytochrome *c* oxidase with bound LM; TX-enzyme, cytochrome *c* oxidase with bound TX.

0006-2960/90/0429-764$02.50/0